MAGNETIC RESONANCE IN CHEMISTRY, VOL. 35, 795–801 (1997)

Anion Radicals of Mono- and Bisfunctionalized [60]Fullerene Derivatives. Evidence for ^{13}C Satellites in their EPR Spectra

V. Brezová,[1] A. Staško,[1]* P. Rapta,[1] D. M. Guldi,[2] K.-D. Asmus[2] and K.-P. Dinse[3]
[1] Department of Physical Chemistry, Slovak Technical University, Radlinského 9, SK-812 37 Bratislava, Slovak Republic
[2] Radiation Laboratory, University of Notre Dame, Notre Dame, Indiana 46446, USA
[3] Physical Chemistry III, TH Darmstadt, D-642 87 Darmstadt, Germany

Upon photo- and electrochemical *in situ* reduction of [60]fullerene derivatives, $C_{60}[C(COOEt)_2]_n$ ($n = 1, 2$), characteristic single-line EPR spectra are observed which are attributable to the corresponding radical anions. Monofunctionalized $C_{60}[C(COOEt)_2]$ shows a reduction behavior similar to pristine C_{60}, i.e. formation of a primary radical A which converts with time into B with a peak-to-peak width of $pp_A \approx 0.1$ mT and $g_A = 2.0000$, $pp_B \approx 0.05$ mT and $g_B = 2.0006$. In contrast, the EPR spectra of the four bis-adducts-{equatorial, *trans*-1, *trans*-2 and *trans*-3 $C_{60}[C(COOEt)_2]_2$} are dominated by only one narrow line with pp ranging from 0.007 to 0.03 mT and g values between 2.0002 and 2.0004. Their relative width changes with the regiosteric positioning of the functionalizing addends. Well resolved spectra reveal ^{13}C satellites, originating from 12–20 carbon nuclei. Slightly higher splittings ($a_{^{13}C} \approx 0.2$ mT) for four carbon nuclei suggest higher spin density at the keto group carbons of the bis(ethoxycarbonyl)methylene substituents. © 1997 John Wiley & Sons, Ltd.

Magn. Reson. Chem. 35, 795–801 (1997) No. of Figures: 6 No. of Tables: 2 No. of References: 48

Keywords: EPR; [60]fullerenes; anion radicals; electron transfer; ^{13}C satellites

Received 20 May 1997; accepted 21 June 1997

INTRODUCTION

Photoinduced electron transfer includes a wide range of processes that are of paramount importance in chemistry and biology. Recent studies regarding the generation of [60]fullerene anions have focused on electron transfer reactions both in the fullerene's ground and excited states.[1] Their identification and characterization have been performed mainly by two different techniques, namely UV–visible–near-IR spectroscopy and EPR spectroscopy.[2–30] Whereas UV–visible–near-IR spectroscopy focuses exclusively on assigning a set of characteristic transition bands to the fullerene's anions,[17–21, 27,28] EPR spectroscopy accounts for more structural relevant parameters of the generated radical anions.[9,16,24,29,30] Originally, C_{60} mono-anions were believed to exhibit a broad EPR line having a peak-to-peak separation (*pp*) frequently larger than 3 mT.[2–14] Conversely, upon *in situ* reduction of [60]fullerene we monitor a primary species **A** with $pp_A = 0.09$ mT and $g_A = 2.0000$. This radical transforms subsequently into **B** with $pp_B = 0.04$ mT and $g_B = 2.0006$.[31,32] With progressing reduction, particularly in less polar solvents and in the presence of large anions, we see a further species **C**, which shows a wide line with $pp_C > 3$ mT and $g_C = 1.998$.[29] This has been rationalized in terms of **A** representing the primary radical species ($C_{60}^{-\bullet}$), **B** depicting a dimeric associate thereof $(C_{60}^{-\bullet})_2$ and **C** probably being a cluster with larger aggregation numbers $(C_{60}^{-\bullet})_n$. Our observation is confirmed by more recent experiments on *in situ* generated $C_{60}^{-\bullet}$, showing narrow EPR lines.[30,33–35] An extremely narrow line ($pp \approx 0.01$ mT) of the fullerene's radical anion was reported from the pulsed EPR experiments.[36]

The polyfunctional structure of buckminsterfullerene, C_{60}, containing 30 reactive double bonds located at the junctions of two hexagons led to the exploration of an extended number of functionalization methodologies.[37–40] Breaking the I_h symmetry of pristine C_{60} leads to small, but nevertheless noticeable, changes of the threefold degenerate molecular orbitals.[41,42] Consequently, a narrowing of the fullerene's EPR lines is expected. In contrast, the mono-anions of [60]fullerene *o*-quinodimethane adducts, reported recently in our[43,44] and other laboratories,[20,45] did not show the expected line narrowing. Instead, a slight line broadening ($pp = 0.105$ mT) relative to pristine [60]fullerene ($pp = 0.09$ mT) was found, which might reflect the unresolved interaction with the methylene protons of the functionalizing addends.[20,45] In the present paper, we describe extremely narrow EPR lines (*pp* down to 0.007 mT) observed during the *in situ* reduction of

---

* *Correspondence to*: A. Staško.

Contract grant sponsor: Slovak Grant Agency; *Contract grant number*: 1/4206/97.
Contract grant sponsor: Volkswagen-Stiftung.
Contract grant sponsor: Office of Basic Energy Sciences of the Department of Energy.

CCC 0749–1581/97/110795–07 $17.50

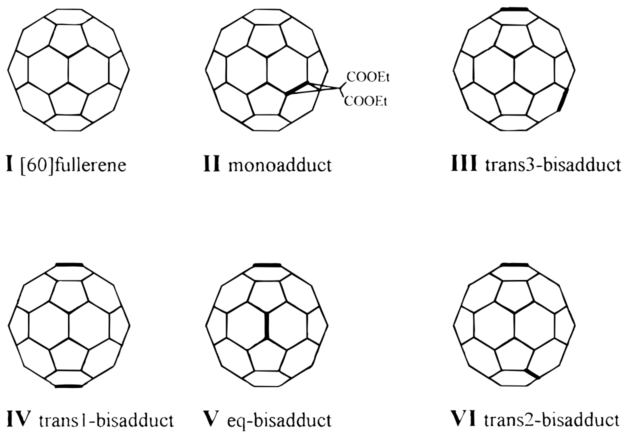

I [60]fullerene **II** monoadduct **III** trans3-bisadduct

IV trans1-bisadduct **V** eq-bisadduct **VI** trans2-bisadduct

Scheme 1. Investigated fullerenes [bold bonds indicate $>C(COOEt)_2$ functionalization].

[60]fullerene bis(ethoxycarbonyl)methylene bis-adducts. These narrow lines facilitate the observation of resolved ^{13}C satellites, which are described and analyzed in detail.

EXPERIMENTAL

The structures of the investigated fullerenes **I–VI** are summarized in Scheme 1. Fullerene (**I**) (gold quality) was obtained from Hoechst (Germany) and the functionalized fullerene derivatives **II–VI** were synthesized according to the literature procedure.[46,47] Toluene, analytical-grade acetonitrile and tetrabutylammonium perchlorate (TBAP) for electrochemical analysis were purchased from Fluka. Dimethyl sulfoxide (DMSO) for gas chromatography (Aldrich) was used. The radical generation was carried out *in situ* under an argon atmosphere in the cavity of a Bruker 200D EPR spectrometer.[31,32,43] The recorded spectra were simulated by an Aspect 2000 computer (Bruker standard program). A medium-pressure mercury lamp (Applied Photophysics, UK) served as the irradiation source. Wavelengths below 300 nm were blocked by a Pyrex filter. For the cathodic reduction experiments a platinum grid was used as the working electrode. It was amperostatically polarized with low currents *vs.* an Ag/AgCl reference electrode which was placed closely to the center of working electrode. This galvanostatic procedure allows better potential control at the entire platinum grid than by conventional potentiostatic techniques. In the latter techniques a considerable potential gradient, particularly at higher currents, is built up along the platinum grid. The corresponding cyclic voltammograms were taken with a platinum wire (surface area 2 mm^2) *vs.* a saturated calomel reference electrode (SCE), equipped with a ferrocene/ferrocenium (Fc/Fc^+) internal potential marker using equipment from Heka (Germany). Near-IR spectra of fullerenes **III** and **VI** (0.25 mM, 0.09 M Et_3N) were recorded with a Nicolet Magna 750 FT-IR spectrophotometer using argon-purged and irradiated solutions.

RESULTS AND DISCUSSION

Photochemical reduction

EPR spectra recorded during the photochemical reduction of fullerenes **I**, **II** and **V** with triethylamine (TEA) as an electron donor in TBAP-saturated (0.09 M TEA and 15 mg ml^{-1} TBAP) toluene solutions are shown in Fig. 1(a)–(c). Reduction of pristine [60]fullerene(**I**)[31,32] and *o*-quinodimethane adducts in CH_3OH, CH_3CN–toluene (1:1, v/v) or DMSO[43,44] revealed the formation of a primary radical product **A** with $pp_A = 0.09$ mT and $g_A = 2.0000$. With progressing irradiation, radical **A** transformed into radical **B** having $pp_B = 0.04$ mT and $g_B = 2.0006$.[31,32,43,44] In neat toluene, generation of transient species **B**, for example of pristine C_{60} (**I**), was observed in much lower yields than in polar solvents [Fig. 1(a)]. Addition of 15 mg ml^{-1} of TBAP to the reaction mixture increased the stability of the formed radicals **A** and **B**.[32] Under analogous conditions, the yield of **A** and **B** using monofunctionalized **II** is much higher than that found for pristine [60]fullerene (**I**) [Fig. 1(a) and (b)].

Remarkable differences were found in the time-resolved reduction of derivatives **III–VI** and **I–II**, as demonstrated in Fig. 1(c) (fullerene **III**). Upon reduction, fullerenes **I** and **II** formed consecutively transient species **A** and **B** whereas functionalized derivatives **III–VI** revealed the immediate formation of a single radical species with a relatively narrow EPR line ($pp < 0.02$ mT) positioned at g values around 2.0002–2.0004 (Fig. 2 and Table 1). It is evident that the EPR spectra are dominated by a characteristic central line with a relative width decreasing in the order **I** > **II** > **III** > **IV** > **V** > **VI** (Table 1). Whereas the spectra of **II–VI** were generated under similar conditions, e.g. using Et_3N as an electron donor, a higher conversion of pristine C_{60} (**I**) to **B** required substitution of Et_3N by TiO_2. It should be noted that the spectrum, which is attributed to species **B**, still indicates a contribution of **A** in Fig. 2. In addition, some non-symmetrically positioned signals (marked with an asterisk) can be seen in Fig. 2 which are apparently not associated to the central line.

A preparative problem should be mentioned here which has a significant impact on the EPR spectra of fullerene derivatives **IV** and **VI**. The low synthetic yields of derivative **IV** and its similar polarity to **VI**[47] might have the consequence that, despite their chromatographic separation, the eluted fraction of **IV** contains **VI** as an admixture. Indeed, the EPR spectrum of $IV^{-\bullet}$, measured at low microwave power (1 mW; standard used for all probes), provides evidence for the presence of $VI^{-\bullet}$. Derivative **VI** was found to saturate more easily than its analogue **IV**. Thus, in order to suppress a strong overlapping contribution of $VI^{-\bullet}$, the EPR spectrum of $IV^{-\bullet}$ (shown in Fig. 2) was recorded at a higher microwave power, namely 100 mW.

Electrochemical reduction

The photochemical reduction was complemented by

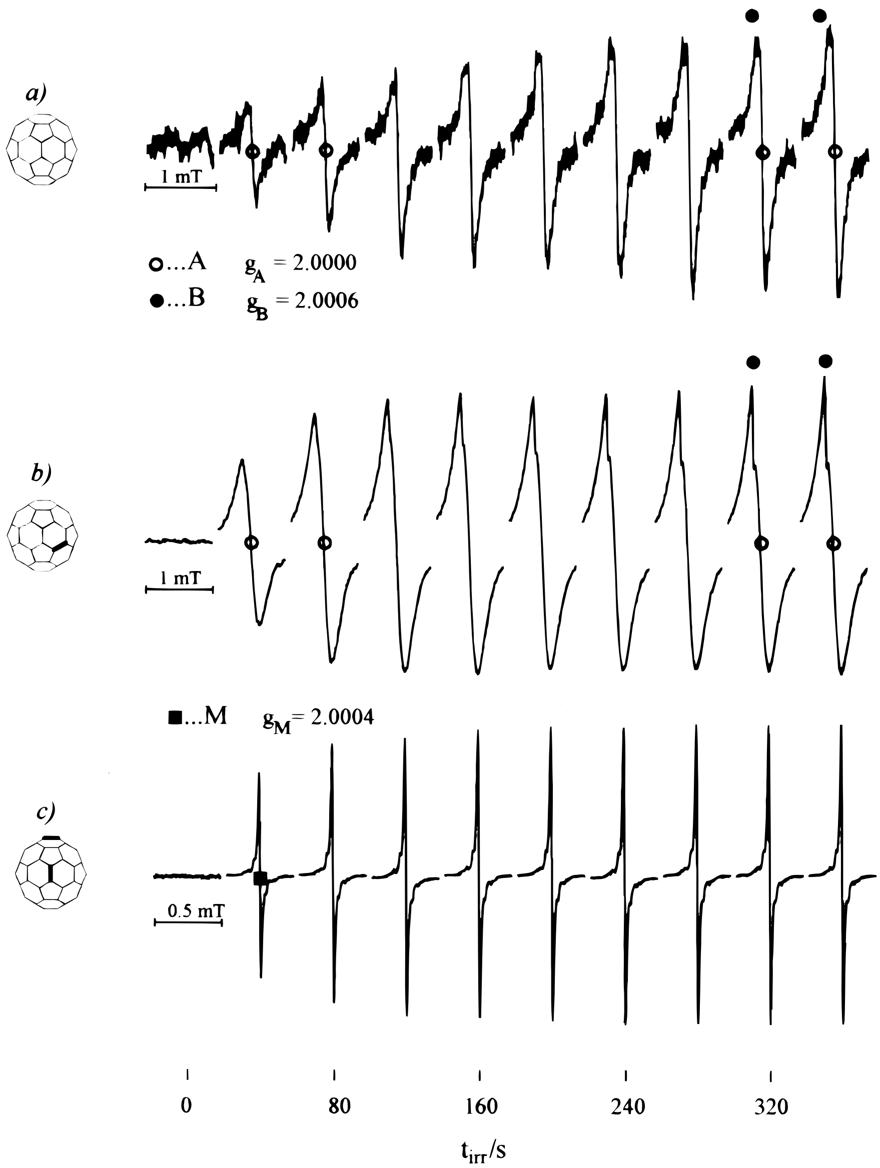

Figure 1. EPR spectra observed during the photochemical generation from 0.25 mM fullerenes, 0.09 M Et_3N, saturated with TBAP in toluene solution with progressing irradiation time: (a) **I**; (b) **II**; (c) **V**.

some cyclic voltammetric measurements in toluene–DMSO (3 : 1, v/v) using 0.1 M TBAP as supporting electrolyte. The data associated with the first and second reduction potentials of fullerenes **I**–**VI** are given in Table 2. The cyclic voltammogram of fullerene derivative **VI**, as shown in Fig. 3, illustrates a nearly reversible behavior for both reduction steps. Simultaneous electrochemical EPR experiments were performed at the potential of the first reduction step. The corresponding EPR spectrum (see inset in Fig. 3) closely resembles that generated in the photochemical studies (Fig. 2). Owing to a better spectral resolution and more convenient generation, the photochemical results are preferentially evaluated in the following sections.

Near-IR measurements

The near-IR spectrum of the fullerene mono-anion of derivative **V** generated under analogous experimental conditions, as stated in the EPR section (Fig. 2), is shown in Fig. 4. A characteristic transition band was recorded with λ_{max} at 1055 nm slightly blue shifted relatively to the previously reported value ($\lambda_{max} = 1065$ nm[46]). This shift probably reflects the different dielectric constant of the solvent. Similarly, using derivative **VI**, the fullerene's characteristic radical anion band was observed at $\lambda_{max} = 1030$ nm. The near-IR data confirm the formation of the corresponding mono-anions and also substantiate the compatibility of our previous pulse radiolysis studies[46] with the current photochemical and electrochemical applications.

^{13}C satellites in EPR spectra

Earlier we reported on the attempt to generate [60]fullerene's radical anion ($C_{60}^{-\bullet}$) of a sample that was ^{13}C enriched (7%).[26,31] The ^{13}C enrichment resulted in a considerable line broadening relative to pristine $C_{60}^{-\bullet}$ ($pp_A = 0.09$ mT), preventing the detection of resolved

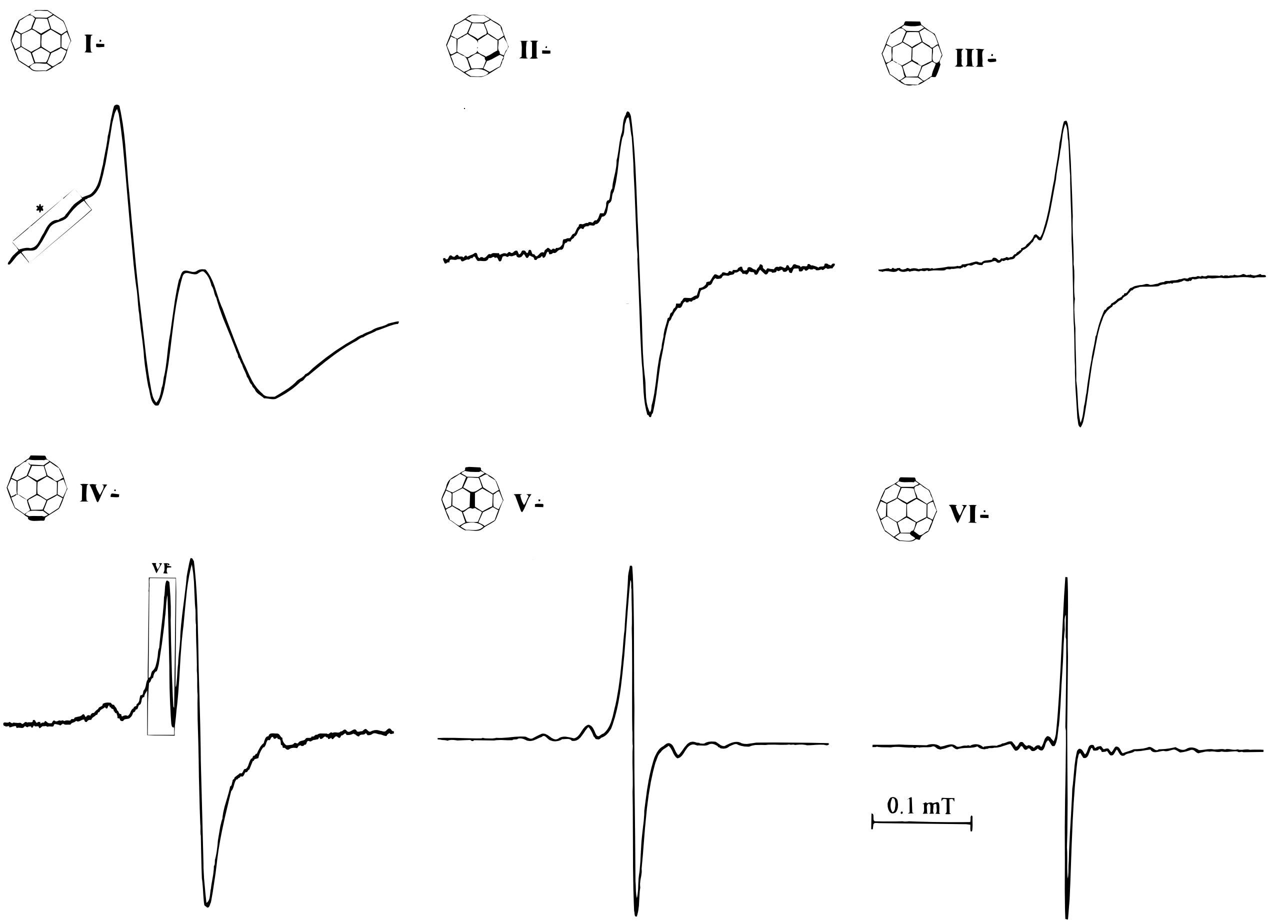

Figure 2. EPR spectra of the photochemically generated [60]fullerene mono-anions (I–VI)$^{-\bullet}$. The spectrum of I$^{-\bullet}$ was obtained in the 0.05 mM [60]fullerene, irradiated for 40 s in toluene–methanol (1 : 1) TiO_2 suspension ($[TiO_2] = 1$ g l^{-1}). The spectra of (II–VI)$^{-\bullet}$ were measured using 0.25 mM fullerene and 0.09 M Et_3N in toluene–DMSO (3 : 1) solutions after irradiation periods of 3 min for II$^{-\bullet}$ and 10 s for (III–VI)$^{-\bullet}$. The hyperfine structure marked with an asterisk originates from other species.

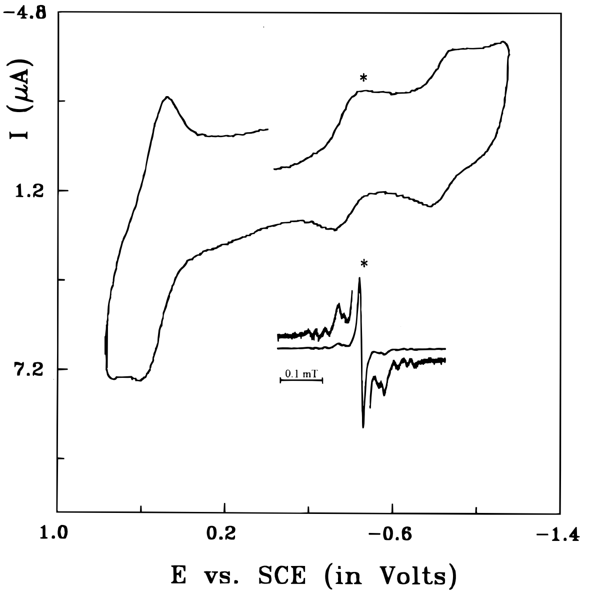

Figure 3. Cyclic voltammogram obtained in 0.25 mM VI, 0.1 M TBAP in toluene–DMSO (3 : 1) solution with Fc/Fc$^+$ reference. * The inset represents the corresponding EPR spectrum observed at the potential of the first reduction peak.

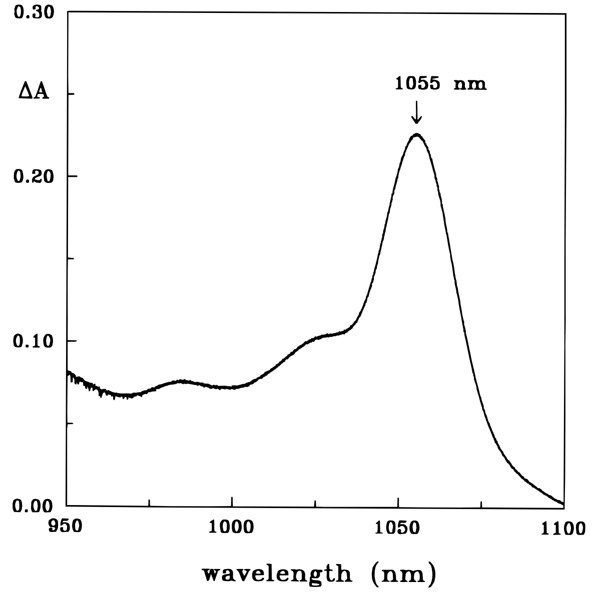

Figure 4. Near-IR spectrum of fullerene mono-anion radical V$^{-\bullet}$ obtained under analogous experimental conditions to those for the EPR investigations in Fig. 2 with an irradiation time of 60 s.

Table 1. The *g* values, peak-to-peak widths (*pp*) and splitting constants of ^{13}C satellites ($a_{^{13}C}$) extracted by simulation from EPR spectra of anion radicals (I–VI)$^{-\cdot}$ [a]

	Central lines		Satellites
Radical	*g*	*pp* (mT)	$a_{^{13}C}$ (mT) (number of carbon nuclei)
$\mathbf{I}^{-\cdot}$	2.0000 (**A**) 2.0006 (**B**)	0.09 0.04	66% **A** 34% **B**
$\mathbf{II}^{-\cdot}$	2.0000 (**A**) 2.0006 (**B**)	0.1 0.027	15% **A** **B** (as central line 50C) $a_{^{13}C}$: 0.09 (14C)
$\mathbf{III}^{-\cdot}$	2.0004	0.019	$a_{^{13}C}$: 0.1934, 0.165, 0.1612, 0.1328 (all 1C); 0.1208, 0.1006, 0.082 (all 2C); 0.0644 (6C) 20% **X**
$\mathbf{IV}^{-\cdot}$	2.0002	0.017	$a_{^{13}C}$: 0.19, 0.0854, 0.0684 (all 4C); 0.02468 (2C) 25% **X**, 12% $\mathbf{VI}^{-\cdot}$
$\mathbf{V}^{-\cdot}$	2.0004	0.01	$a_{^{13}C}$: 0.2188, 0.1796, 0.1738, 0.1690, 0.1484, 0.1348, 0.1328, 0.1182 (all 1C); 0.0830 (6C); 0.0624 (2C) 30% **X**
$\mathbf{VI}^{-\cdot}$	2.0004	0.006	$a_{^{13}C}$: 0.2652, 0.2290, 0.1778, 0.1240, 0.1142 (all 1C); 0.1072 (3C); 0.0840 (4C); 0.0728 (4C); 0.0556 (3C); 0.0420 (1C); 0.0386 (4C); 0.0366 (4C); 0.0240 (1C) 20% **X**, 15% $\mathbf{IV}^{-\cdot}$

[a] The intensity of central lines correspond to 50 carbons (40 for $\mathbf{VI}^{-\cdot}$). Intensities of **X** or $\mathbf{IV}^{-\cdot}$ and $\mathbf{VI}^{-\cdot}$ are given in % of the total spectral intensity.

^{13}C satellites. In the present investigation, very narrow EPR spectra ($pp < 0.02$ mT) of bisfunctionalized compounds **III–VI** indicate the presence of well resolved ^{13}C satellites. These ^{13}C satellites are analyzed by the following simulation.

The time evolution of EPR spectra that are associated with the generation of **A** and **B** of [60]fullerene were treated according to a previous simulation study.[31] Radical species **A** and **B** could be fitted well with Lorentzian lines characterized by the parameters $g_{\mathbf{A}} = 2.0000$, $g_{\mathbf{B}} = 2.0006$, $pp_{\mathbf{A}} = 0.09$ mT and $pp_{\mathbf{B}} = 0.04$ mT. This fitting is also valid for the spectra of **A** and **B** presented here. The central lines were well described with a Lorentzian curve for **I–V**. Only the EPR spectrum of radical $\mathbf{VI}^{-\cdot}$ required application of a Gaussian–Lorentzian (1:1) lineshape. The peak-to-peak widths which were applied in the current simulation are listed in Table 1. In order to complete the simulation of the EPR spectra in Fig. 2, especially to the central line, we accounted for the carbon satellites with splitting constants ($a_{^{13}C}$) and the numbers of ^{13}C nuclei, as specified in Table 1. The lineshape parameters were identical with those of the central line. Additionally, a wide line component **X** with $pp = 1$ mT positioned at the center of the main line was used. The relative intensities of the central and the satellite lines are expressed in number of carbons considered in the simulation (typically about 50C to the central line and around 16C for satellites). The contributions of **X**, $\mathbf{IV}^{-\cdot}$ and $\mathbf{VI}^{-\cdot}$ are expressed relative to the integral intensity of the entire spectrum.

The spectral changes involving the formation of **B** (**II**), as depicted in Fig. 2, could be fitted also by adding a satellite that corresponds to a group of 14 equivalent ^{13}C nuclei with $a_{^{13}C} = 0.09$ mT. Numerous individual lines (Fig. 2) which were poorly resolved complicated the simulation procedure of **III**. An approximate fitting revealed, however, eight groups of satellites with a total of 16 carbons. Their splitting constants are summarized in Table 1.

In contrast, reasonably resolved spectra were obtained for fullerene derivatives **IV–VI**. The simulated spectra are shown for comparison in Fig. 5, and the data which were extracted there from are given in Table 1. The radical species of **IV** revealed 14 carbon nuclei contributing to the satellites. Owing to the high symmetry of **IV** (D_{2h}), these 14 carbons originate from only four groups with 4C, 4C, 4C and 2C. This corresponds well to a relatively high degree of carbon equivalency as evolves from ^{13}C NMR experiments.[47] It is remarkable that the first group has a relatively high splitting constant ($a_{^{13}C} = 0.19$ mT). Since the keto groups of the

Table 2. Half-wave potentials (V) of the first ($E^1_{1/2}$) and second ($E^2_{1/2}$) reduction peaks (*vs.* SCE reference electrode and ferrocene/ferricenium internal potential marker) of the fullerenes I–VI obtained upon cyclic voltammetry in 0.1 M TBAP in toluene–DMSO solutions with a scan rate of 500 mV s^{-1}

Fullerene	$E^1_{1/2}$ *vs.* SCE	Fc/Fc$^+$	$E^1_{1/2}$ *vs.* Fc/Fc$^+$	$E^1_{1/2}$ (probe) $-E^1_{1/2}(C_{60})$ [a]	$E^2_{1/2}$ *vs.* SCE
I	−0.26	0.51	−0.77	—	−0.72
II	−0.31	0.54	−0.85	−0.08	−0.77
III	−0.39	0.54	−0.93	−0.16	−0.84
IV	−0.38	0.54	−0.92	−0.15	−0.82
V	−0.37	0.54	−0.91	−0.14	−0.83
VI	−0.34	0.54	−0.88	−0.11	−0.78

[a] $E^1_{1/2}$ (probe) $- E^1_{1/2}$ (C_{60}) is the potential shift referred to the unsubstituted [60]fullerene.

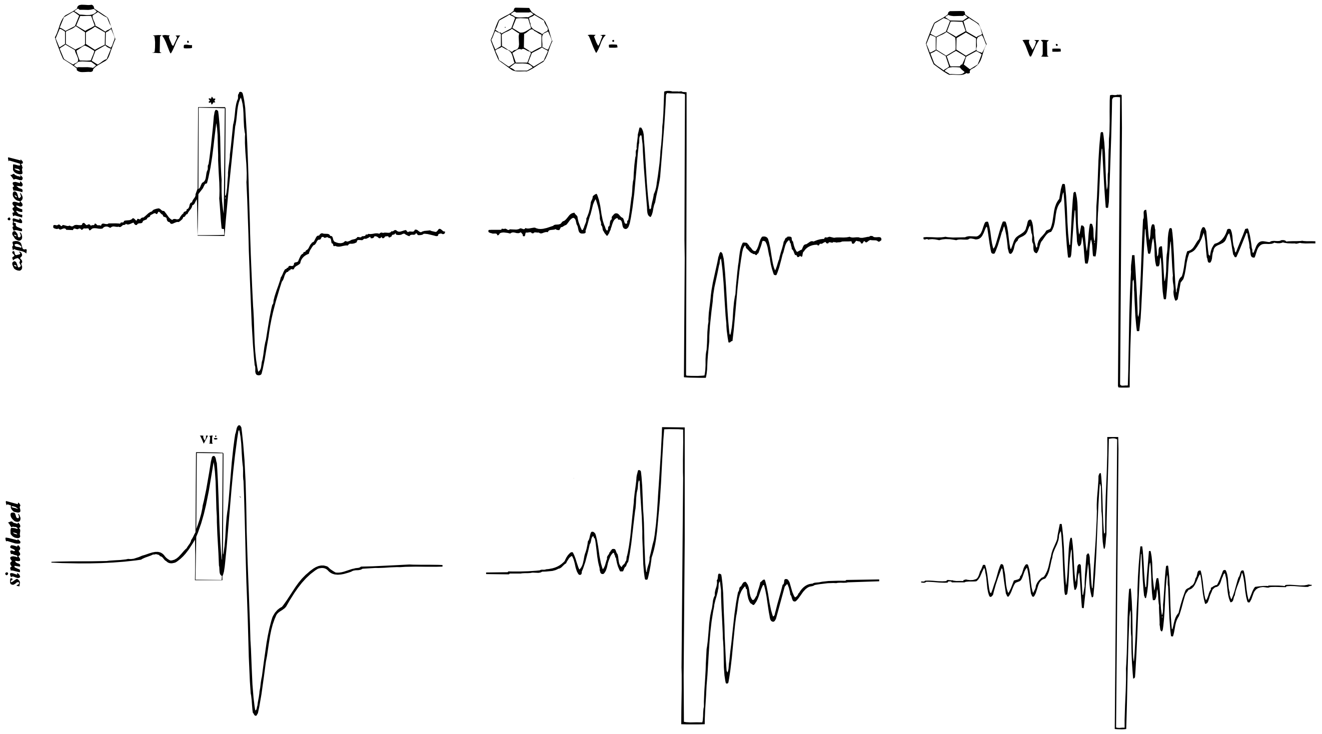

Figure 5. Experimental and simulated EPR spectra of [60]fullerene mono-anions **IV**$^{-\bullet}$, **V**$^{-\bullet}$ and **VI**$^{-\bullet}$ photochemically generated as stated in Fig. 2.

bis(ethoxycarbonyl)methylene addends have much stronger acceptor properties compared with the carbons atoms of the conjugated systems,[48] the four highest splittings probably originate from carbon nuclei of the keto groups.

The radical species that are associated with the reduction of the less symmetric **V** (C_s) and **VI** (C_2) showed considerably more satellites than **IV**. For example, 10 groups and 13 groups of satellites were noticed for **V**$^{-\bullet}$ and **VI**$^{-\bullet}$, respectively. The integral number of carbons contributing to these satellites are, however, similar to those computed for (**II–IV**)$^{-\bullet}$, namely 16C for **V**$^{-\bullet}$ and over 20C for **VI**$^{-\bullet}$ [A larger number of carbon nuclei in ^{13}C satellites and a corresponding smaller contribution of the central line of **VI**$^{-\bullet}$ if compared with (**II–V**)$^{-\bullet}$ results from a considerably better resolution of the spectrum of **VI**$^{-\bullet}$ with $pp = 0.007$ mT.] At least four satellite carbons in the spectra of both **V**$^{-\bullet}$ and **VI**$^{-\bullet}$ show relatively large splitting constants. In analogy with **IV**, this can be rationalized in terms of originating from the carbon atoms located at the keto function of the bis(ethoxycarbonyl)methylene addends. In line with the preparative difficulties mentioned above, the spectrum of **IV**$^{-\bullet}$ evidently contains an admixture of **VI**$^{-\bullet}$ (Fig. 5) and, analogously, simulation reveals the presence of **IV**$^{-\bullet}$ in the spectrum of **VI**$^{-\bullet}$.

Generally, the number of carbons seen by resolved satellites is limited to about 16 nuclei. This suggests that exclusively the carbons in the immediate neighborhood of the keto groups interact noticeably with the unpaired electron.

Acknowledgements

We thank the Slovak Grant Agency, Project 1/4206/97, and the Volkswagen-Stiftung for financial support and the Deutscher Akademischer Austauschdienst (DAAD) for equipment. Part of this work was supported by the Office of Basic Energy Sciences of the Department of Energy (this is contribution No. NDRL-3997 from the Notre Dame Radiation Laboratory).

REFERENCES

1. C. S. Foote, *Top. Curr. Chem.* **169**, 347 (1994).
2. D. Dubois, K. M. Kadish, S. Flanagan, R. E. Haufler, L. P. F. Chibante and L. J. Wilson, *J. Am. Chem. Soc.* **113**, 4364 (1991).
3. D. Dubois, M. T. Jones and K. M. Kadish, *J. Am. Chem. Soc.* **114**, 6446 (1992).
4. W. Koh, D. Dubois, W. Kutner, M. T. Jones and K. M. Kadish, *J. Phys. Chem.* **96**, 4163 (1992).
5. D. Dubois, G. Moninot, W. Kutner, M. T. Jones and K. M. Kadish, *J. Phys. Chem.* **96**, 7137 (1992).
6. M. M. Khaled, R. T. Carlin, P. C. Trulove, G. R. Eaton and S. S. Eaton, *J. Am. Chem. Soc.* **116**, 3465 (1994).
7. P. C. Trulove, R. T. Carlin, G. R. Eaton and S. S. Eaton, *J. Am. Chem. Soc.* **117**, 6265 (1995).
8. S. S. Eaton, A. Kee, R. Konda, G. R. Eaton, P. C. Trulove and R. T. Carlin, *J. Phys. Chem.* **100**, 6910 (1996).
9. S. S. Eaton and G. R. Eaton, *Appl. Magn. Reson.* **11**, 155 (1996).
10. P.-M. Allemand, A. Koch, F. Wudl, Y. Rubin, F. Diederich, M. M. Alvarez, S. J. Anz and R. L. Whetten, *J. Am. Chem. Soc.* **113**, 1050 (1991).
11. Q. Xie, E. Perez-Cordero and L. Echegoyen, *J. Am. Chem. Soc.* **114**, 3978 (1992).
12. A. J. Schell-Sorokin, F. Mehran, G. R. Eaton, S. S. Eaton, A. Viehbeck, T. R. O'Toole and C. A. Brown, *Chem. Phys. Lett.* **195**, 225 (1992).
13. J. Chen, Q.-F. Shao, Z.-E. Huang, R.-F. Cai and S.-M. Chen, *Chem. Phys. Lett.* **235**, 570 (1995).

14. T. Kato, T. Kodama, M. Oyama, S. Okazaki, T. Shida, T. Nakagawa, Y. Matsui, S. Suzuki, H. Shiromaru, K. Yamauchi and Y. Achiba, *Chem. Phys. Lett.* **186**, 35 (1991).
15. R. D. Rataiczak, W. Koh, R. Subramanian, M. T. Jones and K. M. Kadish, *Synth. Met.* **56**, 3137 (1992).
16. M. A. Greaney and S. M. Gorun, *J. Phys. Chem.* **95**, 7142 (1991).
17. T. Kato, T. Kodama and T. Shida, *Chem. Phys. Lett.* **205**, 405 (1993).
18. J. W. Arbogast, C. S. Foote and M. Kao, *J. Am. Chem. Soc.* **114**, 2277 (1992).
19. J. L. Anderson, Y.-Z. An, Y. Rubin and C. S. Foote, *J. Am. Chem. Soc.* **116**, 9763 (1994).
20. M. Baumgarten, A. Gügel and L. Gherghel, *Adv. Mater.* **5**, 458 (1993).
21. A. Z. Sension, G. R. Szarka, G. R. Smith and R. M. Hochstrasser, *Chem. Phys. Lett.* **185**, 179 (1991).
22. J. Stinchcombe, A. Pénicaud, P. Bhyrappa, P. D. W. Boyd and C. A. Reed, *J. Am. Chem. Soc.* **115**, 5212 (1993).
23. P. Bhyrappa, P. Paul, J. Stinchcombe, P. W. D. Boyd and C. A. Reed, *J. Am. Chem. Soc.* **115**, 11004 (1993).
24. P. W. D. Boyd, P. Bhyrappa, P. Paul, J. Stinchcombe, R. D. Bolskar, Y. Sun and C. A. Reed, *J. Am. Chem. Soc.* **117**, 2907 (1995).
25. R. Subramanian, P. Boulas, M. N. Vijayashree, F. D'Souza, M. T. Jones and K. M. Kadish, *J. Chem. Soc., Chem. Commun.* 1847 (1994).
26. J. Friedrich, P. Schweitzer, K.-P. Dinse, P. Rapta and A. Staško, *Appl. Magn. Reson.* **7**, 415 (1994).
27. D. M. Guldi, H. Hungerbühler, E. Janata and K.-D. Asmus, *J. Phys. Chem.* **97**, 11258 (1993).
28. D. M. Guldi, R. E. Huie, P. Neta, H. Hungerbühler and K.-D. Asmus, *Chem. Phys. Lett.* **223**, 511 (1994).
29. A. Staško, V. Brezová, P. Rapta and K.-P. Dinse, *Fullerene Sci. Technol.* **5**, 593 (1997).
30. I. I. Khairullin, W.-T. Chang and L.-P. Hwang, *Fullerene Sci. Technol.* **4**, 423 (1996).
31. A. Staško, V. Brezová, S. Biskupič, K.-P. Dinse, P. Schweitzer and M. Baumgarten, *J. Phys. Chem.* **99**, 8782 (1995).
32. V. Brezová, A. Staško, P. Rapta, G. Domschke, A. Bartl and L. Dunsch, *J. Phys. Chem.* **99**, 16234 (1995).
33. L. Piekara-Sady, A. V. Il'yasov, V. Morozov, J. Stankowski, W. Kempinski and Z. Trybula, *Appl. Magn. Reson.* **9**, 367 (1995).
34. R. Klemt, E. Rodunert and H. Fischer, *Acta Chem. Scand.* **50**, 1050 (1996).
35. A. S. Lobach, N. F. Goldshleger, M. G. Kaplunov and A. V. Kulikov, *Chem. Phys. Lett.* **243**, 22 (1995).
36. M. Bennati, A. Grupp, P. Bäuerle and M. Mehring, *Chem. Phys.* **185**, 221 (1994).
37. F. Wudl, *Acc. Chem. Res.* **25**, 157 (1992).
38. R. Taylor and D. R. M. Walton, *Nature* (*London*) **363**, 685 (1993).
39. F. Diederich and C. Thilgen, *Science* **271**, 317 (1996).
40. A. Hirsch, *Synthesis*, 895 (1995).
41. W. H. Green, Jr, S. M. Gorun, G. Fitzerald, P. W. Fowler, A. Ceulemans and B. C. Titeca, *J. Phys. Chem.* **100**, 14892 (1996).
42. M. Bennati, A. Grupp, M. Mehring, P. Belik, A. Gügel and K. Müllen, *Chem. Phys. Lett.* **240**, 622 (1995).
43. V. Brezová, A. Gügel, P. Rapta and A. Staško, *J. Phys. Chem.* **100**, 16232 (1996).
44. A. Staško, V. Brezová, S. Biskupič, K.-P. Dinse, R. Groβ, M. Baumgarten and A. Gügel, *J. Electroanal.* **423**, 131 (1997).
45. L. Gherghel and M. Baumgarten. *Synth. Met.* **69**, 1389 (1995).
46. D. M. Guldi, H. Hungerbühler and K.-D. Asmus, *J. Phys. Chem.* **99**, 9380 (1995).
47. A. Hirsch, I. Lamparth, H. R. Karfunkel, *Angew. Chem., Int. Ed. Engl.* **33**, 437 (1994).
48. P. Zuman, *Substituent Effects in Organic Polarography*. Plenum Press, New York (1967).